Data-Driven Comparison of Four Cutaneous Displays for Pinching Palpation in Robotic Surgery

Jeremy D. Brown[1], Mary Ibrahim[1], Elyse D. Z. Chase[1], Claudio Pacchierotti[2], and Katherine J. Kuchenbecker[3]

***Abstract*— Current teleoperated surgical robots do not provide surgeons with haptic feedback, due in part to the safety risks associated with grounded kinesthetic forces. Ungrounded cutaneous feedback provides an elegant and inherently stable way to refer haptic feedback to the surgeon in such situations. Choosing the most appropriate display, however, is challenging given the substantial number of unique cutaneous displays presented in the literature. In this work, we demonstrate how measuring the space of tactile sensations that a device can create can be employed to objectively compare different cutaneous displays for a specific task. We built four cutaneous displays and compared their ability to render sensations measured while pinching four disparate materials with a biomimetic tactile sensor. As predicted, quantitative tactile rendering errors varied significantly across devices and materials. The results of this comparison can be used to design better cutaneous displays for pinching palpation in robotic surgery. Furthermore, the proposed approach could provide a useful tool for evaluating novel cutaneous devices for various other tactile tasks, providing an objective framework to supplement and guide future human subject studies.**

I. Introduction

Robotic minimally invasive surgery (RMIS) provides better visualization and dexterity than laparoscopic surgery [1], [2], but clinically available RMIS systems do not enable the surgeon to feel any haptic (kinesthetic or cutaneous) information from the surgical environment. While robotic surgeons have learned to rely on visual feedback for tasks such as dissection and suturing [3], the omission of haptic feedback significantly impedes surgical procedures that require the surgeon to use his or her fingers to localize hard inclusions (typically tumors) or arterial structures within soft tissue.

While full haptic feedback would potentially benefit RMIS, the addition of kinesthetic force feedback carries a significant risk of causing unstable oscillations in the robotic system [4]. Therefore, research has shifted to the alternative approach of *sensory subtraction*, in which the cutaneous portion of the haptic feedback is delivered without the kinesthetic portion [5], [6], [7], [8]. Beyond ensuring stability, cutaneous feedback is appealing because it can be implemented without significant modification of the master interface or the telerobotic slave's motion controller.

Researchers have proposed many different cutaneous display devices, including 2-DoF tilting plate compliance displays [9], 3-DoF planar fingertip displays [10], [6], fabric displays [11], [12], [13], and linkage displays [14]. The utility of each of these devices has been evaluated in one or more human subject studies, but the experiments vary greatly in their procedures, the task studied, and the telerobotic system into which the display was integrated. To our knowledge, no previous study has compared multiple cutaneous displays against one another with the same intended application and experimental setup, making it difficult to know which cutaneous display approach holds the most promise.

We are developing a testbed for comparing different cutaneous displays for pinching palpation feedback in RMIS. Our intended surgical application is pulmonary nodule resection, a thoracic surgical procedure that requires the surgeon to localize and excise tumors from the lung. This procedure is particularly challenging because the lung is deflated during the operation, reducing the utility of any preoperative images. Surgeons doing this procedure through an open incision therefore rely heavily on tactile cues gained from bimanual palpation of the lung, holding it with one hand and pinching it with the other, often discovering non-imaged malignant nodules [15]. While an RMIS approach would beneficially eliminate the need for a thoracotomy to access the lungs, pulmonary nodule resection cannot be performed with current robotic surgery systems due to the lack of haptic feedback. New imaging modalities that make cancerous tissue fluoresce [16] also cannot completely solve this problem because nodules are often deep in the tissue and can become inflamed, thereby distorting the fluorescent image.

Our testbed consists of three major subsystems: a tactile grasper that features a BioTac (SynTouch, LLC) biomimetic sensor on one grasping finger and attaches to the end-effector of a da Vinci surgical robot, a thoracic model that includes phantom lung tissue with simulated embedded tumors, and a pinching interface that consists of various fingertip cutaneous displays that attach to the master controller of a da Vinci surgical robot. We want to determine which device can best display the tactile sensations felt by the BioTac pinching the phantom tissue. To compare these devices fairly, we must actuate each device in a manner that presents to the

*This research was supported by a Technology Research Grant from Intuitive Surgical, Inc.

[1]J. D. Brown, M. Ibrahim, and E. D. Z. Chase are with the Department of Mechanical Engineering & Applied Mechanics, University of Pennsylvania, Philadelphia, PA 19104, USA. {brownjer, maryi, elysec}@seas.upenn.edu

[2]C. Pacchierotti is with the Department of Advanced Robotics, Istituto Italiano di Tecnologia, Via Morego 30, Genova 16163, Italy. claudio.pacchierotti@iit.it

[3]K. J. Kuchenbecker is with the Departments of Mechanical Engineering & Applied Mechanics and Computer & Information Science, University of Pennsylvania, Philadelphia, PA 19104, USA. kuchenbe@seas.upenn.edu

fingertip its best approximation of the sensations measured by the BioTac during pinching. Given that each device has a unique actuation paradigm and particular degrees of freedom, predicting the best actuation pattern is quite difficult. While a skin deformation model could be employed, as done in [17], [18], building these models is time intensive, and the results may not be reliable. Furthermore, a model-based approach also requires one to derive a model that maps BioTac sensations to skin deformations, another difficult task.

On the other hand, a data-driven approach to device actuation has been shown to be both efficient and effective [19], [20]. This approach works by placing the BioTac sensor inside the cutaneous display and recording the sensations the BioTac measures while the display is actuated throughout its entire range of motion. The result is a direct mapping between display actuation and sensor measurements that is inverted during operation, actuating the cutaneous display based on the sensor measurements from the BioTac using a nearest neighbor approach [19], [20]. This approach succeeds partially because it captures the sensations produced by the real device rather than a model of how the device is supposed to work; consequently, we adopt such an approach in this paper. An additional benefit of this mapping is that it makes available every sensation the device could produce as measured by the BioTac. These sensations are expected to differ between devices and therefore offer a basis for objective device comparison. We expect that *the most appropriate device for a given application would be the one that can produce BioTac sensations closest to those sensed by the BioTac during the target task*. Pacchierotti et al. previously showed that the objective error between sensed and actuated tactile sensations correlates well with subjective measures of tactile display quality obtained from a traditional human subject study [19].

This paper asks whether a data-driven approach can be used to objectively compare the performance of multiple cutaneous displays for a selected tactile exploration task. We designed and constructed four different displays for the particular task of pinching palpation. The described approach to comparing cutaneous displays has never before been reported in the literature. If feasible, it could prove useful to researchers designing novel cutaneous displays for a wide range of applications, providing an objective evaluation of the display's rendering capabilities. Such insights might reduce the number of human subject studies that must be conducted to refine and validate a particular tactile display.

II. Methods

This section describes the cutaneous devices we created, the manner in which they were calibrated, and the process by which we recorded pinching palpation data for use in comparing the devices to one another.

A. Cutaneous Display Devices

We developed the four cutaneous displays shown in Fig. 1 as possible candidates for displaying the sensations of pinching palpation in robotic surgery. Two of these devices are

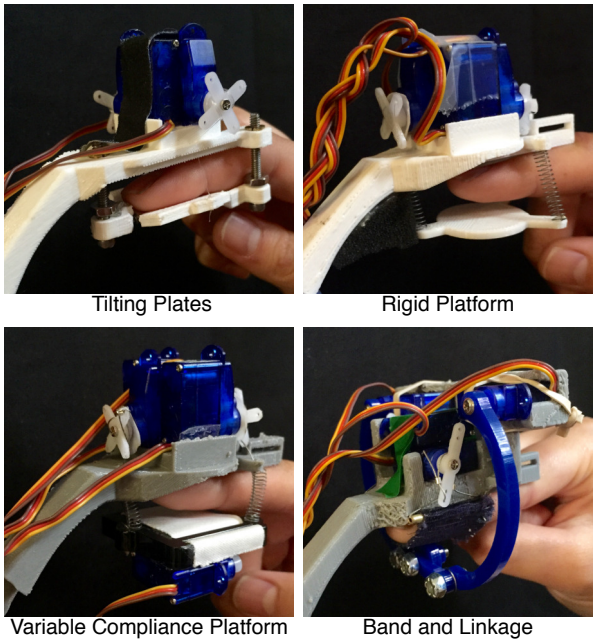

Fig. 1. The four cutaneous display devices.

largely based on displays proposed in the literature, and the other two are novel, based loosely on other devices proposed in the literature. Each device has a different actuation mechanism that produces unique sensations on the finger. A description of each device appears below. All four are actuated by generic analog Sub-Micro Servos purchased from Pololu Corporation (Las Vegas, USA). This servo model has a mass of 3.7 g, measures 20.2 mm $\times$ 20.2 mm $\times$ 8.5 mm, has a stall torque of 0.042 Nm at 6 V, and takes 0.07 s to rotate 60° under no load.

1) Tilting Plates Display: The TP display is a 2-DoF mechanism similar to the device described by Yazdian et al. [9]. It consists of two plates that pivot around axes aligned with and centrally located with the long axis of the finger. Each plate is actuated separately by a servo mounted on a static platform above the finger. Cables connect the servo motor horns to the free end of each plate. By controlling the cable lengths, the motors cause the plates to press on the left and right sides of the fingertip. When both cables are pulled, the plates form a V shape, squeezing on the fingertip from both sides. Torsional springs return the plates to a flat reference configuration when not actuated. The plates are in contact with the fingertip when the cables are fully extended.

2) Rigid Platform Display: The RP display is a 3-DoF parallel mechanism display similar to the one presented by Pacchierotti et al. [21], [22]. It centers on an under-actuated rigid platform whose roll and pitch orientations and vertical translation are controlled by three servos mounted on a static platform above the finger. Cables connect the servo motor horns to extensions from the rigid platform, and linear springs around the cables push the platform toward a reference configuration away from the fingertip when the cables lengthen; the platform does not contact the fingertip

when the cables are fully extended.

3) Variable Compliance Platform Display: The VCP display features a platform whose orientation and vertical translation are controlled by three servos mounted on a static platform above the finger, similar to the RP display. However, the compliance of this platform is actively controlled by a fourth servo, making it a 4-DoF mechanism. The platform is a U-shaped piece of acrylic with a band of white woven fabric placed across the opening. A servo mounted to the bottom of the platform tensions the fabric through a cable. A brass pipe is sewn into the fabric at both ends to provide even pulling and tensioning upon actuation. Varying the tension in the cable varies the compliance of the fabric. This device was inspired by the variable compliance fabric display of Bianchi et al. [11]. Linear springs around the cables of the platform push the platform toward a reference configuration when not actuated; the platform does not contact the fingertip when the cables are fully extended.

4) Band and Linkage Display: The BL display is a 4-DoF device composed of two separate 2-DoF mechanisms. The first mechanism consists of a band of fabric that wraps around the fingerpad; taken from a headband, the fabric has a patterned rubber coating that prevents it from slipping against the finger. To provide even pulling and tensioning upon actuation, a brass pipe is sewn into either end of the fabric band, and a cable runs through each pipe and is attached to a servo. Pulling on the fabric with both servo motors creates sensations of tightening around the fingertip. Pulling with only one servo motor creates shear stresses on the fingertip. The second mechanism is a five-bar linkage driven by two additional servo motors mounted on the static platform. A round disk is mounted at the center of the moving part of the linkage; this disk can press into the fingertip through the fabric to simulate the feel of a lump. A short cable connects the other two moving pivots to prevent the linkage from falling into configurations that provide no contact with the finger. This device was inspired by the fabric band display of Minamizawa et al. [13] and the five-bar linkage of Tsetserukou et al. [14]. The fabric and linkage are in contact with the fingertip when the cables are fully extended.

B. BioTac Tactile Sensor

The SynTouch BioTac is a biomimetic tactile sensor that closely resembles the human fingertip in shape, stiffness, and multimodal sensory capabilities [23], [24], [25]. It includes a rigid core patterned with 19 active electrodes and 4 ground electrodes, a green rubber external skin, conductive fluid between the core and the skin, a fingernail, and associated electronics. Contact with an object deforms the skin and the conductive fluid, thereby changing the impedance between each of the 19 electrodes and ground and giving an estimate of finger shape. A hydro-acoustic pressure sensor measures both the DC pressure and the AC pressure of the conductive fluid. The BioTac is internally heated to about 37°C (human body temperature), and a thermistor on the surface of the rigid core records both the DC temperature and the AC temperature.

C. Cutaneous Device Calibration

To objectively compare the four above-mentioned cutaneous displays, we recorded the full set of BioTac sensations that each device can produce. Each data set was gathered using the calibration method originally reported by Pacchierotti et al. [21] and then also used in [19], [20]. As shown in Fig. 2, the BioTac was placed inside the cutaneous device, in the same way a human user would wear it. Moreover, in order to better match tactile sensations experienced during RMIS, each cutaneous display was mounted in a 3D-printed bracket that held the display in an orientation similar to how it would be held when operated at the da Vinci master controller. The actuated elements of the display were then moved to a wide range of configurations, and the effect of each of these configurations was registered on the BioTac; we saved both the commanded motor angles of each pose and the resulting effect that pose had on the tactile sensor. Since our focus is in sensing deformations, we consider the 19 electrode impedance readings and the DC pressure signal. This calibration procedure was repeated for the four devices described in Sec. II. Given their different designs and ranges of motion, each device is expected to create a different set of sensations.

BioTac communication and data logging were provided by a custom Robot Operating System (ROS) package [26]. The servo motors were controlled using a Phidget 1061 8-motor servo board. When connected to the Phidget board, each servo motor had a safe operating range of motion of 160°. As discussed in [19], using a small motor step size during calibration helps a system achieve higher rendering performance. However, running the calibration with a very small step size can take a very long time. Using a step size of 3° in a device with three actuators would yield $148,877$ unique actuation configurations, requiring approximately 47 hours for the calibration to complete [19]. To achieve good sampling resolution while limiting the calibration time, we chose a step size of 10°, which is not far from the 9° step size successfully used in previous work [19]. The end-effector was held in each configuration for 0.3 s, and the values gathered by the BioTac during that time period were arithmetically averaged.

Including the time to move between actuation configurations, calibration required approximately 1 s for each unique configuration that was tested. Using a step size of 10° for the TP display's two servo motors yielded $\left(\frac{160°}{10°}\right)^2 = 256$ unique actuation configurations, taking approximately five minutes for the calibration to complete. Using a step size of 10° for the three servo motors on the RP display yielded $\left(\frac{160°}{10°}\right)^3 = 4,096$ unique actuation configurations, taking approximately one hour. A step size of 10° was also used for the three servo motors actuating the platform of the VCP device, but a larger step size of 40° was chosen for the servo motor actuating the fabric tension. This choice reduced the calibration duration by reducing the number of unique actuation configurations from $\left(\frac{160°}{10°}\right)^4 = 65,536$

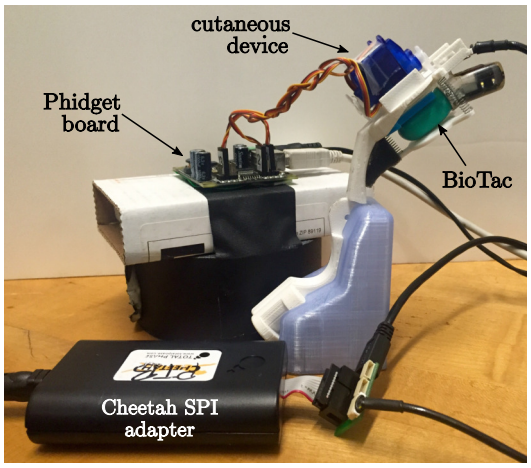

Fig. 2. Calibration setup featuring the BioTac mounted in the rigid plate cutaneous display. The BioTac is connected to the computer through a Cheetah high-speed SPI adaptor, and the servo motors are controlled through a Phidget servo board.

to $\left(\frac{160°}{10°}\right)^3 \times \left(\frac{160°}{40°}\right)^1 = 16,384$. This calibration took approximately four hours to complete, and it produced four unique platform compliances for each unique 3-DoF platform configuration. A step size of 10° was used for the four servo motors of the BL display. However, the five-bar linkage limited the range of motion of its two servo motors to 50°. We had therefore $\left(\frac{160°}{10°}\right)^2 \times \left(\frac{50°}{10°}\right)^2 = 6,400$ unique actuation configurations to consider, taking approximately two hours for the calibration to complete. To ensure that the calibration was successful, the mapping from motor commands to BioTac sensations was inverted and each display was actuated according to sensations measured by the BioTac using a nearest neighbor search routine. A video of the rendering for each display can be found in the supplemental material for this paper.

The sensations that the display induces during calibration are recorded by the BioTac as points in 20-dimensional space (19 electrode impedances + DC pressure), with each measurement recorded on a 12-bit scale (0 – 4095) at 100 Hz. To account for drift in the BioTac readings over time, we zeroed each set of calibration readings by subtracting what the BioTac felt when the servos were not activated; the remaining readings thus represent the differential sensations that occur when the servos are activated. A similar zeroing technique was used by [27].

D. Principal Component Analysis (PCA)

While the BioTac's perceptual space has twenty dimensions, each display has only two, three, or four degrees of freedom. Therefore, a principal component analysis can be applied to the BioTac calibration data to visualize the sensations provided by each device in a lower-dimensional space. Fig. 3 shows how the electrodes and DC pressure contribute to the most important principal components for each device; we chose to show only the principal components that explain more than 2% of the variance in the calibration data.

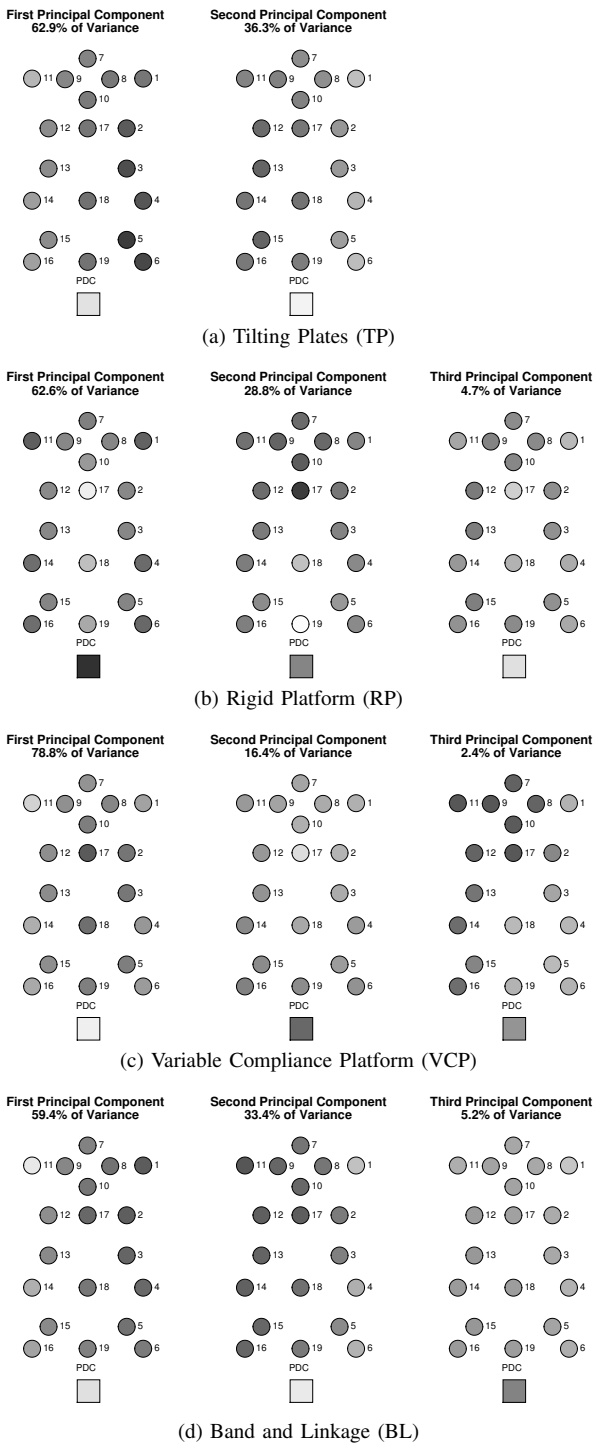

Fig. 3. Graphical depiction of the principal components needed to capture the variations seen in each device's calibration data. Each numbered circle represents an electrode on the surface of the BioTac's rigid core, while the central square stands for DC pressure. Sensors colored similarly tend to positively correlate with one another in that principal component, while sensors colored opposite one another (light vs. dark) tend to negatively correlate with one another.

The spatial representation of the electrode layout in Fig. 3 corresponds to the spatial representation of the electrodes on the BioTac.

For the 2-DoF TP display, the first two components

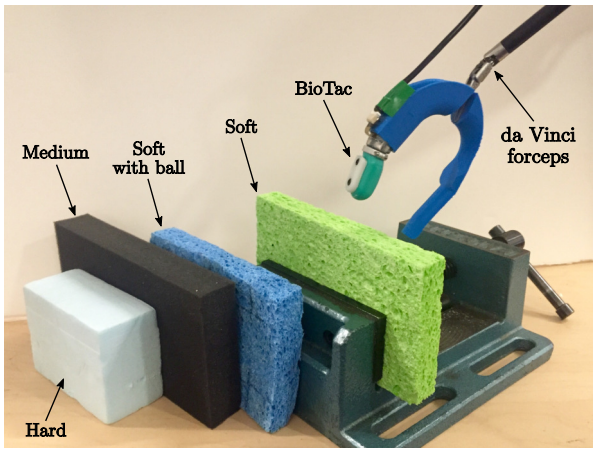

Fig. 4. Experimental setup for collection of pinching palpation data. A BioTac is mounted to an Intuitive da Vinci instrument and used to squeeze different materials.

account for 99.2% of the variance in the BioTac calibration data, and they spatially align with the left and right sides of the BioTac, as we expected from the bilateral design of this device. For the 3-DoF RP display, the first three components account for 96.1% of the variance in the BioTac calibration data; the first component indicates center/side characteristics, the second shows both front/back and center/side characteristics, while the third shows the electrodes and DC pressure moving together. For the 4-DoF VCP display, the first three components account for 97.6% of the variance in the BioTac calibration data. Although this is a 4-DoF device, the fourth principal component explains less than 2% of the variance. The first VCP principal component indicates mainly center/side characteristics, while the second shows activation of all electrodes and DC pressure together, and the third shows strong left/right and front/back characteristics. For the 4-DoF BL display, the first three components account for 98% of the variance in the BioTac calibration data. Again, the fourth component had little to contribute in explaining the variance. The first two components seem to show contact on the left and right sides of the sensor, while the third component shows collective activation. As hypothesized, the different devices create rather different sets of sensations on the BioTac; what remains to be seen is which device is best suited to the task of pinching palpation.

E. Pinching Palpation Data

We would like to discover how well each cutaneous display can mimic the feel of pinching different materials, as would be encountered during pinching palpation in RMIS. Thus we collected pinching palpation data with the BioTac attached to one side of an EndoWrist ProGrasp™ grasper via a custom 3D printed adapter. A rigid finger extension was attached to the other side of the grasper to provide equal and opposite pinching forces on the material. This pinching system was attached to a da Vinci Standard surgical robot and operated by one of the experimenters. Three different materials were selected for this experiment, including pale blue hard foam (Hard), dark gray medium foam (Medium), and a soft green sponge (Soft) that is thought to closely approximate the feel of deflated lung tissue. Additional data was collected from an otherwise-identical blue soft sponge that was embedded with a 0.25-in. diameter steel ball bearing to simulate a tumor (Soft with ball). The entire setup is shown in Fig. 4, along with the selected material samples.

Seven data recordings were taken for each of the four material samples. During each recording, the material was pinched with the entire BioTac, the left side of the BioTac, the right side of the BioTac, and only the tip of the BioTac (by pinching the edge of the material). The experimenter performed both a hard and soft pinch at each of the BioTac orientations, resulting in eight pinches per recording. For the sponge with ball bearing, pinching data at the tip of the BioTac was not collected because the ball bearing was fixed in the sponge and could not be moved to the edge. For this material alone, the final two pinches repeated the pattern of pinching with the full BioTac. To account for drift in the BioTac's readings over time, each recording was zeroed by subtracting out the average sensation experienced for 0.1 s of time when the BioTac was known not to be touching anything. The remaining readings in each recording thus represent the differential sensations experienced by the BioTac during that particular interaction.

III. Results

As a measure of tactile rendering fidelity, we calculated the error $\bar{e}_f$ between the 20-dimensional zeroed tactile sensation $\boldsymbol{s}$ registered by the BioTac when squeezing the sample and the closest 20-dimensional zeroed tactile sensation $\boldsymbol{s_r}$ that the selected device could render, chosen from the BioTac data collected during that device's calibration. Error $\bar{e}_f$ is calculated as the mean over time of the Euclidean distance between these two vectors,

$$\bar{e}_f = \frac{1}{K}\sum_{k=1}^{K}\left(\sqrt{\sum_{i=1}^{20}(s_i - s_{r,i})^2}\right), \tag{1}$$

where K is the total number of samples recorded for the selected interaction. Lower error values indicate a better match between the desired tactile sensations and the rendered tactile sensations.

Fig. 5 shows the DC pressure (PDC) data for a sample interaction with the Soft material. In addition to the time history of the sensed PDC value, the plot shows the time history of the PDC value that each device would apply on a BioTac placed inside the cutaneous device. One can see that all four devices are able to increase the pressure in the sensor, but they match its value to varying degrees because of their unique actuation paradigms, and because the rendering algorithm also considers the values of the 19 electrode impedances. Fig. 6 shows the time history of the error (PDC and electrodes combined, calculated via (1)) for a different sample interaction with the Medium material; an ideal device would match every sensation perfectly, yielding zero error at all points in time.

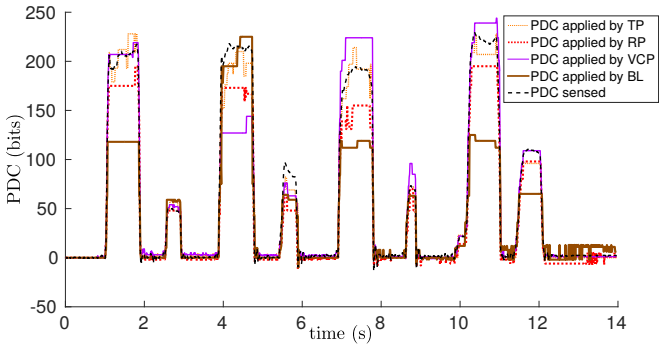

Fig. 5. Experimental evaluation. DC pressure (PDC) data registered by the BioTac during a representative interaction with the Soft material. Each increase in sensed PDC shows one of the eight pinches included in the test. At each time step, each cutaneous device attempts to present the tactile sensations measured at the remote environment.

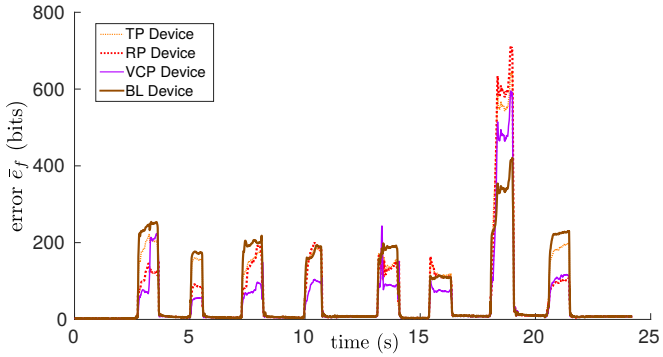

Fig. 6. Experimental evaluation. Error $\bar{e}_f$ registered during a representative interaction with the Medium material. At each time step, each cutaneous device attempts to present the tactile sensations measured while the BioTac pinched the material.

Fig. 7 depicts the average tactile rendering error for the four devices and four materials. To compare the ability of the different devices to render tactile interactions with the considered materials, we ran a two-way repeated-measures ANOVA on the error data shown in Fig. 7. Each tactile interaction was considered as an independent observation. Materials and devices were treated as within-subject factors. Data were subjected to a log transformation to stabilize variance. All the data passed the Shapiro-Wilk normality test. Mauchly's Test of Sphericity indicated that the assumption of sphericity had not been violated for the materials, while it was violated for the devices ($\chi^2(5) = 11.881$, p = 0.04). A Greenhouse-Geisser correction was applied to the tests involving data that violate the sphericity assumption. The ANOVA test revealed statistically significant changes in error due to both the materials (F(3, 18) = 28.077, $p < 0.001$, partial $\eta^2 = 0.824$) and the devices (F(2.019,12.113) = 179.028, $p < 0.001$, partial $\eta^2 = 0.968$). Moreover, there was a statistically significant two-way interaction between materials and devices (F(9,54) = 19.340, $p < 0.001$). Post hoc analysis with Bonferroni adjustments revealed a significant change in the rendering error between Hard and all other materials (Hard vs. Medium, p = 0.002; Hard vs. Soft, $p < 0.007$; Hard vs. Soft with ball, p = 0.005) and between all

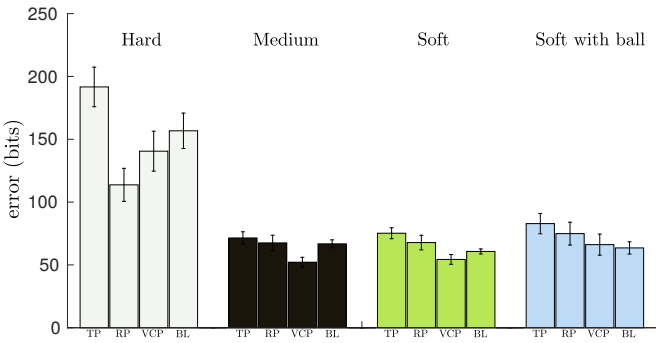

Fig. 7. Experimental evaluation. Average rendering error for each combination of device and material (mean ± standard error of the mean).

pairs of devices except BL vs. RP (TP vs. RP, $p < 0.001$; TP vs. VCP, $p < 0.001$; TP vs. BL, $p < 0.001$; RP vs. VCP, $p = 0.003$; VCP vs. BL, $p = 0.001$). These results were confirmed via analysis of simple main effects.

IV. Discussion and Conclusion

This paper sought to determine whether a data-driven approach can be used to objectively compare the performance of multiple cutaneous displays for a chosen type of tactile interaction. Specifically, we used a BioTac biomimetic sensor to measure the space of sensations produced by four different cutaneous displays as well as the sensations caused by pinching four different materials. The resulting error between the real and rendered sensations allows for an objective comparison of the displays' rendering capabilities.

Overall, our findings highlight the utility and limitations of each display. In particular, none of the four displays presented in this paper can produce the sensations of pinching the Hard material as well as it can emulate the feel of the three other materials. Likewise, the sensations of interacting with the three softer materials (Medium, Soft, Soft with ball) were rendered with similar errors. This distinction highlights the fact that these displays were designed to render the compliance of soft tissue within the body, such as lung tissue and tumors. The servo motors used in all four devices are lightweight and limited in their torque output, so they struggle to render interactions with hard surfaces. Still, each display had different degrees of freedom and actuation paradigms, and as predicted certain displays performed better than the others.

The TP display produced errors that were significantly larger than the RP, VCP, or BL display, suggesting that the TP display is the least ideal of the four. This is not surprising given that the TP display is simplest, with only two degrees of freedom. The VCP display on the other hand produced the smallest error of the four displays, suggesting that it is capable of producing sensations closest to those measured by the BioTac pinching the material. The VCP display featured the same three degrees of freedom as the RP display, but its fourth degree of freedom allowed it to present different levels of compliance for any given orientation and vertical position of the platform. The sensations produced by the RP

and BL displays in general are better than the TP display but not as good as the VCP display and did not significantly differ from each other.

While the VCP display performed better than the RP display for the Medium, Soft, and Soft with ball materials, the RP display performed better than the other three displays for the Hard material. Pinching the Hard material is very similar to pinching a rigid flat surface. The RP display produces tactile sensations with a rigid platform; therefore it was able to produce sensations that were closer to pinching the Hard material than the other three displays. The largest errors were for the TP display, which features two rigid plates that produce tactile sensations by pressing into the sides of the finger. This sensation is very different from the target sensation with the hard material. The VCP display features a platform like the RP display; however, even when actuated, the fabric in the platform cannot become as rigid as the RP display. Still, the sensations produced by the VCP are closer to the RP display than the BL display. While the BL display can produce a pulling sensation on the fingertip, the band wraps around the entire finger and generates sensations on the sides of the BioTac that are more akin to the TP display than either the VCP or RP displays.

While the Hard, Medium, and Soft materials demonstrate how the displays perform when rendering the tactile sensations from pinching a variety of materials, it is the Soft with ball material that is closest to our intended application of lung tissues with tumors. Thus the performance of the displays for this material is of particular interest. Our results demonstrate that the BL display is no better than the VCP display for the Soft with ball material. The BL display, however, was designed to create lump-like sensations on the fingertip. This finding suggests that the BL display was not effective in creating a lump-like sensation that matches what the BioTac sensed in the Soft with ball material. This mismatch most likely stems from the fact that the lump created by the BL display is one size and can move only laterally across the finger, but not forward/backward. The sensations produced by the linkage may also be masked by the fabric band.

While the data-driven approach presented in this paper allows for an objective comparison of multiple cutaneous displays, there are a few areas that could be improved upon. First, the data upon which the comparisons were made highly depends on the calibration routine used to generate the data. For this paper, we used a minimum step size of 10°. A smaller step size would improve the rendering performance of the displays and potentially decrease the corresponding error. Second, we compared only four different materials. The comparison could potentially produce entirely different results if different materials were chosen. Finally, this approach reveals only the theoretical error between the sensations measured by the BioTac pinching real materials and the closest sensations rendered by our displays during calibration. Although this error was previously demonstrated to correlate with perceived rendering quality in a human subject study [19], other factors will affect the experience of a human user, such as the size and shape of the user's fingertip, as well as stimulation of the sensory receptors on the back side of the human finger. Still, while research suggests that the BioTac is indeed a good model for the finger's sensing capabilities [24], [25], the true benchmark of tactile display performance remains user-centric perceptual evaluations.

Despite these limitations, we have successfully demonstrated that one can objectively compare multiple tactile displays using quantitative data gathered with a biomimetic tactile sensor. We believe these comparisons may be useful for evaluating cutaneous displays prior to running human subject studies, allowing critical improvements to be made on the basis of substantive data showing how well the device performs in rendering the sensations for a selected tactile exploration task. While our purpose was to evaluate each of these displays for pinching palpation in RMIS, the approach would work for any other application where the sensor used in the tactile exploration task can fit inside the cutaneous display.

Acknowledgments

We thank Dr. Sunil Singhal from the University of Pennsylvania for advising us on the challenges of robotic pulmonary nodule resection. We thank Intuitive Surgical, Inc., for donating the da Vinci robot and instruments that were used in this research.

References

[1] G. H. Ballantyne, "Robotic surgery, telerobotic surgery, telepresence, and telementoring. Review of early clinical results." *Surgical Endoscopy*, vol. 16, no. 10, pp. 1389–402, 2002.

[2] G. Guthart and J. Salisbury, "The Intuitive telesurgery system: overview and application," in *Proc. IEEE International Conference on Robotics and Automation.*, 2000, pp. 618–621.

[3] M. E. Hagen, J. J. Meehan, I. Inan, and P. Morel, "Visual clues act as a substitute for haptic feedback in robotic surgery," *Surgical Endoscopy and Other Interventional Techniques*, vol. 22, no. 6, pp. 1505–1508, 2008.

[4] N. Diolaiti, G. Niemeyer, F. Barbagli, and J. Salisbury, "Stability of haptic rendering: Discretization, quantization, time delay, and coulomb effects," *IEEE Transactions on Robotics*, vol. 22, no. 2, pp. 256–268, 2006.

[5] D. Prattichizzo, C. Pacchierotti, and G. Rosati, "Cutaneous force feedback as a sensory subtraction technique in haptics," *IEEE Transactions on Haptics*, vol. 5, no. 4, pp. 289–300, 2012.

[6] L. Meli, C. Pacchierotti, and D. Prattichizzo, "Sensory subtraction in robot-assisted surgery: fingertip skin deformation feedback to ensure safety and improve transparency in bimanual haptic interaction." *IEEE Transactions on Biomedical Engineering*, vol. 61, no. 4, pp. 1318–27, 2014.

[7] W. McMahan, J. Gewirtz, D. Standish, P. Martin, J. A. Kunkel, M. Lilavois, A. Wedmid, D. I. Lee, and K. J. Kuchenbecker, "Tool contact acceleration feedback for telerobotic surgery," *IEEE Transactions on Haptics*, vol. 4, no. 3, pp. 210–220, 2011.

[8] K. Bark, W. McMahan, A. Remington, J. Gewirtz, A. Wedmid, D. I. Lee, and K. J. Kuchenbecker, "In vivo validation of a system for haptic feedback of tool vibrations in robotic surgery." *Surgical Endoscopy*, vol. 27, no. 2, pp. 656–64, 2013.

[9] S. Yazdian, A. J. Doxon, D. E. Johnson, H. Z. Tan, and W. R. Provancher, "Compliance display using a tilting-plate tactile feedback device," in *Proc. IEEE Haptics Symposium*, 2014, pp. 13–18.

[10] D. Prattichizzo, F. Chinello, C. Pacchierotti, and M. Malvezzi, "Towards wearability in fingertip haptics: a 3-dof wearable device for cutaneous force feedback," *IEEE Transactions on Haptics*, vol. 6, no. 4, pp. 506–16, 2013.

[11] M. Bianchi and A. Serio, "Design and characterization of a fabric-based softness display," *IEEE Transactions on Haptics*, vol. 8, no. 2, pp. 152–163, 2015.

[12] F. Kimura, A. Yamamoto, and T. Higuchi, "Development of a 2-DOF softness feeling display for tactile tele-presentation of deformable surfaces," *In Proc. IEEE International Conference on Robotics and Automation*, pp. 1822–1827, 2010.

[13] K. Minamizawa, S. Fukamachi, H. Kajimoto, N. Kawakami, and S. Tachi, "Gravity grabber: wearable haptic display to present virtual mass sensation," in *ACM SIGGRAPH 2007 Emerging Technologies*, Aug. 2007, p. 8.

[14] D. Tsetserukou, S. Hosokawa, and K. Terashima, "LinkTouch: A wearable haptic device with five-bar linkage mechanism for presentation of two-dof force feedback at the fingerpad," in *Proc. IEEE Haptics Symposium*, feb 2014, pp. 307–312.

[15] R. J. Cerfolio, A. S. Bryant, T. P. McCarty, and D. J. Minnich, "A prospective study to determine the incidence of non-imaged malignant pulmonary nodules in patients who undergo metastasectomy by thoracotomy with lung palpation," *The annals of thoracic surgery*, vol. 91, no. 6, pp. 1696–700; discussion 1700–1, 2011.

[16] D. Holt, O. Okusanya, R. Judy, O. Venegas, J. Jiang, E. DeJesus, E. Eruslanov, J. Quatromoni, P. Bhojnagarwala, C. Deshpande, S. Albelda, S. Nie, and S. Singhal, "Intraoperative near-infrared imaging can distinguish cancer from normal tissue but not inflammation." *PloS ONE*, vol. 9, no. 7, p. e103342, 2014.

[17] C. Pacchierotti, F. Chinello, M. Malvezzi, L. Meli, and D. Prattichizzo, "Two finger grasping simulation with cutaneous and kinesthetic force feedback," in *Haptics: Perception, Devices, Mobility, and Communication SE-34*, ser. Lecture Notes in Computer Science, P. Isokoski and J. Springare, Eds. Springer Berlin Heidelberg, 2012, vol. 7282, pp. 373–382.

[18] B. Gleeson, S. Horschel, and W. Provancher, "Design of a fingertip-mounted tactile display with tangential skin displacement feedback," *IEEE Transactions on Haptics*, vol. 3, no. 4, pp. 297–301, 2010.

[19] C. Pacchierotti, D. Prattichizzo, and K. J. Kuchenbecker, "Displaying sensed tactile cues with a fingertip haptic device," *IEEE Transactions on Haptics*, vol. 8, no. 4, pp. 384–396, 2015.

[20] ——, "Cutaneous feedback of fingertip deformation and vibration for robotic surgery," *IEEE Transactions on Biomedical Engineering*, vol. 63, no. 2, pp. 278–287, 2016.

[21] ——, "A data-driven approach to remote tactile interaction: From a BioTac sensor to any fingertip cutaneous device," in *Haptics: Neuroscience, Devices, Modeling, and Applications*, ser. Lecture Notes in Computer Science, M. Auvray and C. Duriez, Eds. Springer Berlin Heidelberg, 2014, vol. 8618, pp. 418–424.

[22] C. Pacchierotti, L. Meli, F. Chinello, M. Malvezzi, and D. Prattichizzo, "Cutaneous haptic feedback to ensure the stability of robotic teleoperation systems," *The International Journal of Robotics Research*, vol. 34, no. 14, pp. 1773–1787, Oct. 2015.

[23] N. Wettels and G. E. Loeb, "Haptic feature extraction from a biomimetic tactile sensor: Force, contact location and curvature," in *Proc. IEEE International Conference on Robotics and Biomimetics (ROBIO)*, 2011, pp. 2471–2478.

[24] M. Arian, C. Blaine, G. Loeb, and J. Fishel, "Using the BioTac as a tumor localization tool," in *Proc. IEEE Haptics Symposium*, 2014, pp. 443–448.

[25] J. A. Fishel and G. E. Loeb, "Sensing tactile microvibrations with the BioTac: Comparison with human sensitivity," in *Proc. IEEE International Conference on Biomedical Robotics and Biomechatronics*, 2012, pp. 1122–1127.

[26] "BOLT haptics project." [Online]. Available: http://bolt-haptics.seas.upenn.edu/index.php/Main/HomePage

[27] J. Hui and K. Kuchenbecker, "Evaluating the BioTac's ability to detect and characterize lumps in simulated tissue," in *Haptics: Neuroscience, Devices, Modeling, and Applications*, ser. Lecture Notes in Computer Science, M. Auvray and C. Duriez, Eds. Springer Berlin Heidelberg, 2014, vol. 8619, pp. 295–302.